Diagn Interv Radiol 2026; DOI: 10.4274/dir.2026.263636

ABDOMINAL IMAGING

ORIGINAL ARTICLE



# Multimodality characterization of lipid-poor adenomas: diagnostic performance of computed tomography, magnetic resonance imaging, and 18F-fluorodeoxyglucose positron emission tomography/computed tomography

Sait Kayalı[1]
Sahib Alizada[1]
İbrahim Halil Akkış[1]
Elif Nur Koçak[1,2]
Güney Deniz[3]
Emine Göknur Işık[3]
Merve Gülbiz Dağoğlu Kartal[1]
Şükrü Mehmet Ertürk[1]

[1]İstanbul University, İstanbul Faculty of Medicine, Department of Radiology, İstanbul, Türkiye

[2]Sultangazi District Health Center, Department of Public Health, İstanbul, Türkiye

[3]İstanbul University, İstanbul Faculty of Medicine, Department of Nuclear Medicine, İstanbul, Türkiye

**Corresponding author:** Sahib Alizada

**E-mail:** sahib.alizade.12@gmail.com

Received 10 September 2025; revision requested 24 October 2025; last revision requested 18 January 2026; accepted 25 February 2026.

Epub: 18.03.2026

Publication date:

DOI: 10.4274/dir.2026.263636

**PURPOSE**

Adrenal lesions exhibit a wide spectrum of imaging features, and overlap between benign and malignant entities may complicate diagnosis. This study aimed to evaluate the diagnostic performance of 18F-fluorodeoxyglucose positron emission tomography (PET)/computed tomography (CT), CT, and magnetic resonance imaging (MRI) in the characterization of adrenal lesions, with particular emphasis on lipid-poor adenomas.

**METHODS**

In this retrospective study, 559 adrenal lesions from 477 patients (2012–2024) were analyzed. Lesions were evaluated using PET/CT, unenhanced/contrast-enhanced CT attenuation, and chemical-shift MRI signal changes, based on data availability. Lipid-poor adenomas were defined as lesions with unenhanced CT attenuation > 10 Hounsfield units and no significant signal loss on chemical-shift MRI.

**RESULTS**

The mean maximum standardized uptake value (SUVmax) for lipid-poor adenomas was 4.73 ± 1.78, which was significantly higher than the 3.13 ± 1.15 observed in the non-lipid-poor group ($P$ = 0.002). Similarly, the adrenal-to-liver SUVmax ratio was significantly elevated in the lipid-poor group (1.62 ± 0.52) compared with the non-lipid-poor group (1.19 ± 0.31) ($P$ = 0.009). The optimal cut-off value was determined as 8.4 for lipid-poor lesions and 5.4 for non-lipid-poor lesions, supporting the necessity of lesion-specific thresholds in adrenal characterization.

**CONCLUSION**

Lipid-poor adenomas are metabolically more active and exhibit higher SUVmax values than non-lipid-poor adenomas. Different modalities should be considered when evaluating lipid-poor adenomas. PET/CT is highly sensitive for malignancy detection but may yield false positives in lipid-poor adenomas.

**CLINICAL SIGNIFICANCE**

Accurate differentiation of lipid-poor adenomas from malignant adrenal lesions is essential to avoid unnecessary surgery and invasive procedures. Our findings indicate that a multimodality imaging approach combining PET/CT, CT, and MRI improves diagnostic reliability, reduces misclassification, and supports optimal clinical decision-making.

**KEYWORDS**

Adrenal lesion, adrenal adenoma, adrenal metastasis, lipid-poor adenoma, computed tomography, magnetic resonance imaging, positron emission tomography/computed tomography, maximum standardized uptake value

You may cite this article as: Kayalı S, Alizada S, Akkış İH, et al. Multimodality characterization of lipid-poor adenomas: diagnostic performance of computed tomography, magnetic resonance imaging, and 18F-fluorodeoxyglucose positron emission tomography/computed tomography. *Diagn Interv Radiol*. 18 March 2026 DOI: 10.4274/dir.2026.263636 [Epub Ahead of Print].

Adrenal lesions detected incidentally during imaging studies performed for unrelated indications are referred to as "adrenal incidentalomas." With the widespread use of cross-sectional imaging, the prevalence of incidentalomas has increased to approximately 4%–6% in the general population and rises further with age, reaching 7%–10% in individuals aged > 70 years.[1-3] Given their potential for malignancy, accurate characterization of adrenal lesions is clinically essential.[4] To this end, computed tomography (CT), magnetic resonance imaging (MRI), and positron emission tomography (PET)/CT are commonly used to differentiate benign from malignant lesions.[5]

Adrenal adenomas typically demonstrate low attenuation values on unenhanced CT [< 10 Hounsfield units (HU)], whereas metastatic and other malignant lesions generally show higher attenuation.[6] However, the identification of lipid-poor adenomas remains challenging because their attenuation characteristics on unenhanced CT often overlap with those of malignant lesions. In such cases, contrast-enhanced CT with washout analysis may provide additional diagnostic value.[7] Washout CT is particularly useful in indeterminate lesions with attenuation values > 10 HU. Pathologically atypical adrenal adenomas are also more likely to exhibit atypical imaging features, including larger size, lobulated margins, heterogeneous appearance, and increased attenuation on unenhanced CT, all of which may further complicate differentiation from malignancy.[8]

Owing to its high diagnostic performance in adrenal lesion evaluation, 18F-fluorodeoxyglucose (FDG) PET/CT has become a widely used modality, particularly for distinguishing malignant from benign lesions. Meta-analyses have reported pooled sensitivity and specificity values of 97% and 91%, respectively, for PET/CT in this setting.[5] Malignant adrenal lesions typically demonstrate intense FDG uptake, reflecting increased metabolic activity.[9] However, when using single-phase contrast-enhanced CT alone, differentiation between adrenal metastases and adenomas may be limited, as metastases can exhibit attenuation values similar to those of adenomas, thereby reducing diagnostic accuracy.[10]

In adrenal lesion assessment, an unenhanced CT attenuation threshold of 10 HU is widely accepted due to its high specificity (approaching 100%) for lipid-rich adenomas. Nevertheless, in lipid-poor adenomas with attenuation values exceeding this threshold, chemical-shift MRI techniques offer important additional diagnostic information.[11,12] Chemical-shift MRI is a highly sensitive and specific method for evaluating intracellular lipid content, which is a hallmark feature of adrenal adenomas. The presence of intracytoplasmic lipid enables reliable differentiation of adenomas from metastatic lesions and, in most cases, obviates the need for invasive diagnostic procedures.[3,9,13] Accordingly, adrenal adenomas on MRI are primarily characterized based on their intracellular lipid content.[14]

Although generally accepted standardized uptake value (SUV) threshold values (3.7–5) for differentiating malignant lesions are widely reported in the literature, the lack of specific threshold recommendations that differ according to the lipid content of the lesion constitutes a significant gap in clinical evaluation. In this study, we aim to evaluate the relationship between FDG uptake on PET/CT, lipid content assessed by chemical-shift MRI, and attenuation values obtained from contrast-enhanced and unenhanced CT in adrenal lesions and to investigate the combined contribution of these imaging modalities to clinical diagnosis.

**Main points**

- Lipid-poor adenomas exhibit significantly higher metabolic activity (mean SUVmax: 4.73 ± 1.78) compared to non-lipid-poor adenomas (mean SUVmax: 3.13 ± 1.15) on 18F-FDG PET/CT.
- A dual-threshold interpretation strategy is necessary for differentiating metastases from adenomas; the optimal SUVmax cutoff shifts from 5.4 for non-lipid-poor lesions to 8.4 for lipid-poor lesions.
- The adrenal-to-liver SUVmax ratio (ALR) provides high diagnostic accuracy, with optimal thresholds identified as 1.8 for non-lipid-poor and 2.6 for lipid-poor groups.
- Lipid-poor adenomas pose a significant diagnostic challenge as their higher FDG uptake can mimic malignancy, frequently exceeding standard clinical PET thresholds.

## Methods

### Study design and population

This retrospective study included 477 patients, with a total of 559 adrenal lesions, who were evaluated between 2012 and 2024. All patients underwent FDG PET/CT imaging as part of their clinical assessment. The maximum SUV (SUVmax) values were measured for each adrenal lesion.

Because of the retrospective nature of the study, PET/CT data were analyzed in the form available in the institutional archive. Not all patients underwent both contrast-enhanced and unenhanced CT acquisitions. Accordingly, attenuation values were recorded from the CT component of PET/CT scans, whether contrast-enhanced or unenhanced, depending on availability. The SUV measurements were consistently obtained from PET images corrected using the corresponding CT data. The CT examinations, therefore, included both unenhanced and contrast-enhanced scans. Lesion attenuation values were measured on both contrast-enhanced and unenhanced PET/CT images when available.

MRI examinations were evaluated for signal intensity changes between in-phase and opposed-phase sequences, and fat ratios were calculated quantitatively (Figure 1).

### Definition of lipid-poor adenoma

Lipid-poor adenomas were defined as adrenal lesions with unenhanced CT attenuation values > 10 HU and without significant signal loss on chemical-shift MRI sequences.[15]

### Sample size and patient selection

All patients evaluated at the İstanbul University Faculty of Medicine, Department of Nuclear Medicine, between 2012 and 2024 who were found to have adrenal lesions on FDG PET/CT were eligible for inclusion. PET/CT examinations were performed for metabolic characterization in patients with suspected malignancy and for staging purposes in patients with known malignancy. Adrenal adenomas included in this study were incidentally detected lesions.

### Imaging techniques

### Positron emission tomography/computed tomography protocol

All patients were instructed to fast for ≥ 6 hours prior to 18F-FDG administration. Blood glucose levels were measured before tracer injection, and patients with glucose levels < 200 mg/dL received an intravenous injection of 18F-FDG at a dose of 0.1–0.2 mCi/kg. PET/CT imaging was performed approximately 60 minutes after injection with patients in the supine position.

Image acquisition was performed using two different systems based on the study period. Between 2012 and 2018, images were acquired using a Siemens Biograph TruePoint PET/CT scanner (Siemens Healthineers, Forchheim, Germany). Subsequent examinations were performed using a GE Discovery IQ PET/CT scanner (GE Healthcare).

Low-dose CT scans were obtained using tube voltages of 120–140 kV and a tube current of 50 mA. Following CT acquisition, PET images were acquired from the vertex to the mid-thighs over 6–8 bed positions, with an acquisition time of 3 minutes per bed position. A CT-based attenuation correction was applied to all emission images.

Reconstruction methods differed between the two systems. Images obtained from the Siemens Biograph TruePoint were reconstructed using an ordered-subset expectation maximization algorithm (2 iterations, 8 subsets) with a 5-mm filter. Images obtained from the GE Discovery IQ were reconstructed using a Bayesian penalized likelihood reconstruction algorithm (Q.Clear; $\beta$ = 300). All data were transferred to an Advantage Workstation (version 4.7, GE Healthcare) for visual and quantitative evaluation.

### Magnetic resonance imaging protocol

All MRI examinations were performed using a 1.5-Tesla scanner (MAGNETOM Aera, Siemens Healthcare, Erlangen, Germany). Imaging protocols included conventional and advanced sequences based on clinical indication. Standard MRI sequences consisted of axial T1-weighted gradient-echo imaging [fast low-angle shot (FLASH), in-phase and opposed-phase], coronal T1-weighted FLASH sequences, axial and coronal T2-weighted images, and fat-suppressed sequences (short tau inversion recovery or spectral adiabatic inversion recovery). Diffusion-weighted imaging with corresponding apparent diffusion coefficient maps was also obtained.

For lesion characterization, in-phase and opposed-phase gradient-echo sequences were used to assess intracellular lipid content. When indicated, post-contrast T1-weighted images were acquired following intravenous administration of a gadolinium-based contrast agent at a dose of 0.1 mmol/kg body weight, using fat-suppressed axial and coronal planes.

### Data collection and image analysis

All imaging data and clinical information were obtained retrospectively from the hospital's imaging archive and hospital information management system. The PET/CT images were independently reviewed by two nuclear medicine physicians with ≥ 2 years of experience, and imaging findings related to adrenal lesions were recorded. For normalization, the adrenal-to-liver ratio (ALR) was calculated by dividing adrenal SUVmax by liver SUVmax. A 3 cm spherical region of interest was placed in homogeneous right hepatic lobe parenchyma, carefully avoiding vascular structures, biliary ducts, and focal lesions.

The MRI examinations were independently reviewed by two radiologists with ≥ 2 years of experience, and relevant imaging features were documented.

Adrenal lesion characterization was performed by evaluating CT attenuation values, MRI-derived fat ratios, and PET/CT metabolic parameters.

### Ethics approval

Ethical approval for this study was obtained from the İstanbul University Faculty of Medicine Clinical Research Ethics Committee (approval number: 3229109, date: 11.03.2025).

### Inclusion and exclusion criteria

Patients aged ≥ 20 years who underwent adrenal MRI and 18F-FDG PET/CT between

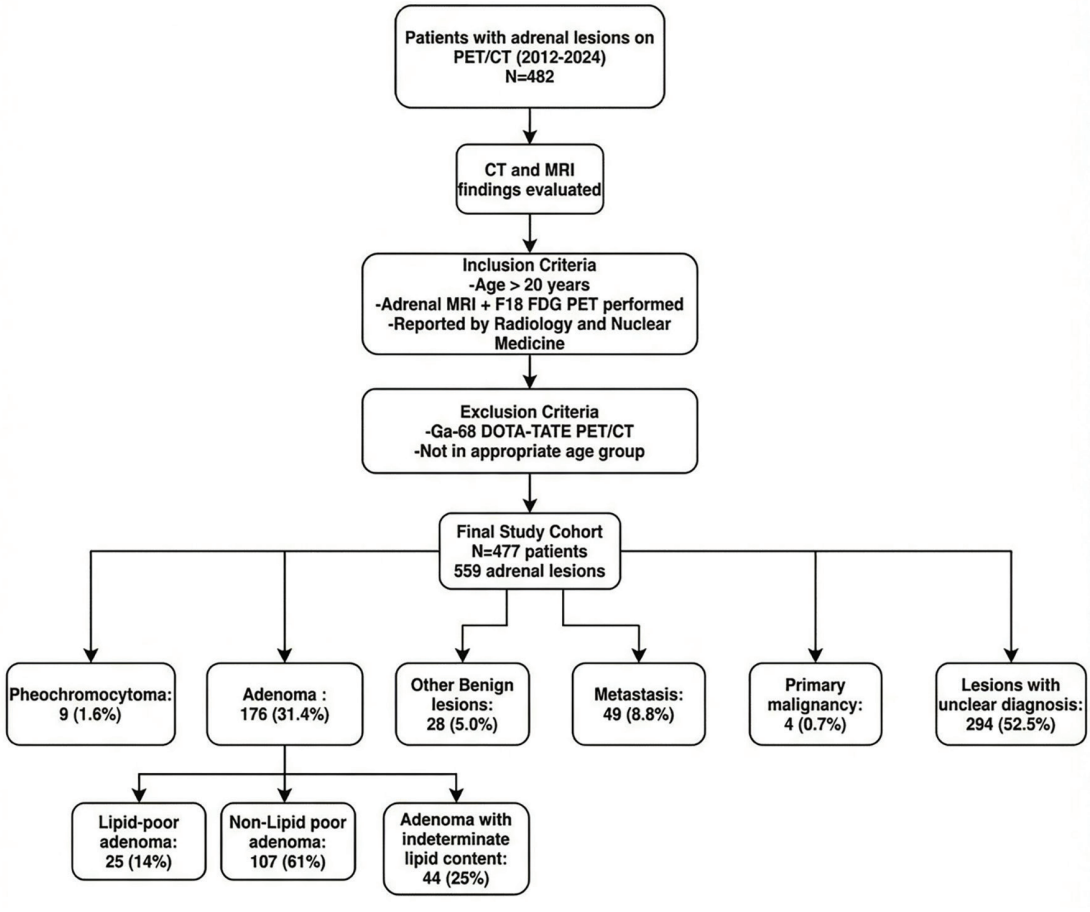


**Figure 1.** Study flowchart. PET/ CT, positron emission tomography/computed tomography; MRI, magnetic resonance imaging; FDG, fluorodeoxyglucose.

2012 and 2024 and were reported to have adrenal lesions by the Departments of Radiology and Nuclear Medicine at İstanbul University Faculty of Medicine were included.

Patients who underwent 68Ga-DOTATATE PET/CT imaging and those who did not meet the age criteria were excluded from the study.

### Statistical analysis

Descriptive statistics were expressed as mean ± standard deviation for continuous variables and as frequency (n) and percentage (%) for categorical variables. The Shapiro–Wilk test was used to assess the normality of continuous data. For comparisons among multiple independent groups, one-way analysis of variance was performed for normally distributed variables, and the Kruskal–Wallis test was used for non-normally distributed variables. In cases where significant differences were detected in either test, post-hoc pairwise comparisons were conducted using Bonferroni-corrected tests. For comparisons between two independent groups, Student's t-test was used for normally distributed data, and the Mann–Whitney U test was applied for non-normally distributed data.

Receiver operating characteristic (ROC) curve analysis was performed to determine optimal cut-off values, with the Youden index used to identify the optimal threshold. A *P* value of < 0.05 within a 95% confidence interval was considered statistically significant. All statistical analyses were performed using IBM SPSS Statistics software (version 30.0; IBM Corp., Chicago, IL, USA).

## Results

A total of 477 patients were included in the study, comprising 559 adrenal lesions. Of these lesions, 29.3% were bilateral, 24.7% were located in the right adrenal gland, and 46.0% were located in the left adrenal gland. The distribution of adrenal lesion pathologies is summarized in Table 1. Overall, adenomas accounted for 31.4% of all lesions, of which 14% were classified as lipid-poor adenomas.

A significant overall difference was also observed among groups for the out-of-phase/in-phase ratio. Subgroup analysis revealed statistically significant differences between adenomas and other benign lesions, primary malignancy, metastases, and pheochromocytomas ($P < 0.003$). Lesion size also differed significantly among groups. Post-hoc analysis demonstrated adenomas were significantly smaller than other benign lesions, metastases, and pheochromocytomas ($P < 0.003$). The SUVmax values showed a significant overall difference between lesion groups ($P < 0.003$). Subgroup analysis revealed significantly higher SUVmax values in metastases (19.90 ± 12.73) than in other benign lesions (5.36 ± 2.60), adenomas (3.60 ± 1.44), and pheochromocytomas (9.46 ± 5.83). Consistently, mean SUVmax values and lesion diameters were higher in patients with primary malignancy and metastases than in other lesion groups (Table 2).

The analysis specifically focused on FDG-avid adenomas (SUVmax > 0) to refine the differentiation between lipid-poor and non-lipid-poor adenomas. Statistical analysis revealed significant differences in PET/CT uptake values between adenoma subtypes. Lipid-poor adenomas exhibited significantly higher metabolic activity than non-lipid-poor adenomas. Specifically, the mean SUVmax for lipid-poor adenomas was 4.73 ± 1.78, which was significantly higher than the 3.13 ± 1.15 observed in the non-lipid-poor group ($P = 0.002$). Similarly, the adrenal-to-liver SUVmax ratio was significantly elevated in the lipid-poor group (1.62 ± 0.52) compared with the non-lipid-poor group (1.19 ± 0.31) ($P = 0.009$) (Table 3).

Using ROC curve analysis, an optimal SUVmax threshold of 5.5 was determined to differentiate all adenomas from metastatic lesions. Additionally, an adrenal-to-liver

**Table 1.** Distribution of adrenal lesion pathologies

| Pathology | n (%) |
|---|---|
| Lesions with unclear diagnosis | 293 (52.5%) |
| Other benign lesions | 28 (5.0%) |
| Adenoma (total) | 176 (31.4%) |
| • Lipid-poor adenoma | 25 (14%) |
| • Non-lipid-poor adenoma | 107 (61%) |
| • Adenoma with indeterminate lipid content | 44 (25%) |
| Primary malignancy | 4 (0.7%) |
| Metastasis | 49 (8.8%) |
| Pheochromocytoma | 9 (1.6%) |

**Table 2.** Comparison of radiological measurements among maximum standardized uptake value avid lesion groups

| Variable | 1. Other benign (Mean ± SD) | 2. Adenoma (Mean ± SD) | 3. Primary malignancy (Mean ± SD) | 4. Metastasis (Mean ± SD) | 5. Pheochromocytoma (Mean ± SD) | *P* | Post-hoc comparison ($P < 0.003$) |
|---|---|---|---|---|---|---|---|
| Size (mm) | 56 ± 48 | 23 ± 13 | 119 ± 54 | 80 ± 50 | 69 ± 45 | < 0.001* | 1-2, 1-3, 1-4, 2-3, 2-4, 2-5 |
| Non-contrast CT (HU) | Median: 13<br>Min: −70<br>Max: 60 | Median: 1<br>Min: −100<br>Max: 41 | Median: 36<br>Min: 32<br>Max: 39 | Median: 32<br>Min: 19<br>Max: 46 | Median: 35<br>Min: 13<br>Max: 37 | < 0.001^ | 1-4, 2-4, 2-5 |
| Contrast enhanced CT (HU) | Median: 36<br>Min: 20<br>Max: 81 | Median: 32<br>Min: −77<br>Max: 117 | Median: 55<br>Min: 45<br>Max: 64 | Median: 46<br>Min: 25<br>Max: 82 | Median: 79<br>Min: 23<br>Max: 105 | 0.004^ | 2-5 |
| SUVmax (Early) | 5.36 ± 2.60 | 3.60 ± 1.44 | 17.20 ± 13.61 | 19.90 ± 12.73 | 9.46 ± 5.83 | < 0.001* | 1-4, 2-3, 2-4, 4-5 |
| Out-of-phase/in-phase ratio | 0.85 ± 0.24 | 0.37 ± 0.20 | 0.94 ± 0.03 | 0.98 ± 0.09 | 0.98 ± 0.05 | < 0.001* | 2-1, 2-3, 2-4, 2-5 |

Statistical analysis: *ANOVA test with Bonferroni correction for multiple comparisons; ^Kruskal–Wallis Test with Bonferroni correction for multiple comparisons. Min, minimum; Max, maximum; CT, computed tomography; HU, Hounsfield units; SUVmax, maximum standardized uptake value; ANOVA, analysis of variance; SD, standard deviation.

SUVmax ratio cut-off of 1.8 was identified for the entire cohort. Subgroup analyses revealed a distinct dual-threshold pattern for differentiating metastases based on lipid content. The optimal SUVmax cut-off was 8.4 for lipid-poor adenomas, whereas it was 5.4 for non-lipid-poor adenomas. Regarding the ALR, the optimal thresholds were identified as 2.6 for the lipid-poor group and 1.8 for the non-lipid-poor group. These results indicate that diagnostic cut-offs significantly shift depending on the lesion's lipid characteristics (Table 4).

## Discussion

Our study specifically demonstrates that lipid-poor adenomas consistently show higher FDG uptake than non-lipid-poor adenomas. This finding indicates that lipid-poor adenomas possess a distinct metabolic profile, which may mimic malignancy on PET/CT and thereby create a diagnostic dilemma in adrenal lesion characterization. This retrospective analysis of 559 adrenal lesions confirms that lipid-poor adenomas (14% of our adenoma cohort) pose the greatest diagnostic overlap with malignant lesions. Our findings indicate that SUVmax provides strong diagnostic utility in differentiating adenomas from metastatic adrenal lesions. The identified cut-off value of 5.5 yielded high sensitivity and specificity, suggesting that this threshold may serve as a practical reference point in the evaluation of indeterminate adrenal masses.

The increased FDG uptake observed in lipid-poor adenomas may be attributed to relatively higher cellular density and glucose metabolism than in non-lipid-poor adenomas. Although a lower SUVmax threshold of 3.7 is commonly used in the literature for malignancy detection, our findings suggest that this value lacks sufficient specificity for this particular subgroup. Instead, we propose a dual-threshold interpretation strategy for differentiation from metastases. Our study demonstrates that the optimal SUVmax cut-off for identifying metastases was 8.4 for non-lipid-poor lesions, compared with 5.4 for lipid-poor lesions. This significant difference between the two groups directly supports our study's hypothesis, suggesting that diagnostic thresholds must be tailored to the lipid content of the lesion.[4]

Previous studies have reported discrimination between adrenocortical tumors versus malignant tumor SUVmax thresholds ranging from approximately 3.1 to 4.3, and several publications have proposed 3.7 as a practical cut-off value due to its high sensitivity, reaching up to 96%, albeit with more limited specificity of approximately 83%.[16] Lower diagnostic thresholds are particularly valuable in a screening context, as even subtle increases in FDG uptake may reliably identify lesions that warrant further diagnostic work-up. With increasing unenhanced CT attenuation of adrenal lesions, the probability of definitive adenoma characterization using chemical-shift MRI progressively diminishes. Notably, this likelihood declines to approximately 33.3% in lesions demonstrating attenuation values > 30 HU, implying that alternative imaging techniques may be more appropriate beyond this cut-off. A prior study demonstrated a statistically significant positive correlation between SUVmax and CT attenuation values in a cohort of 57 adrenal adenomas. Furthermore, it has been reported that increased FDG uptake may be observed in both benign and malignant adrenal lesions. A comprehensive understanding of the FDG uptake patterns of adrenal lesions is therefore essential for improving diagnostic accuracy and refining the differential diagnosis of adrenal masses.[15,17,18] Our findings are consistent with this literature while further demonstrating that these thresholds are insufficient for confidently differentiating lipid-poor adenomas from malignant adrenal lesions.

From a clinical perspective, accurate characterization of adrenal lesions is essential for guiding patient management. Misclassification of benign lesions as malignant may result in unnecessary surgery or biopsy, with associated risks and costs, whereas failure to identify malignant disease may delay potentially life-saving treatment. Although FDG PET/CT demonstrates high sensitivity and

**Table 3.** Comparison of radiological measurements among maximum standardized uptake value in avid adenoma lesion groups

| Variables | Non-lipid-poor adenoma (Mean ± SD) | Lipid-poor-adenoma (Mean ± SD) | *P* value |
|---|---|---|---|
| Size (Maximum diameter, mm) | 25.18 ± 14.36 | 18.04 ± 9.97 | 0.007* |
| Non-contrast CT density (HU) | Median: −2<br>Min: −101<br>Max: 9 | Median: 21<br>Min: 10<br>Max: 41 | <0.001^ |
| Contrast enhanced CT density (HU) | Median: 30<br>Min: −77<br>Max: 94 | Median: 52<br>Min: 5<br>Max: 117 | 0.002^ |
| Chemical shift (Out-of-phase/in-phase ratio) | 0.35 ± 0.19 | 0.46 ± 0.16 | 0.012* |
| SUVmax (Early) | 3.13 ± 1.15 | 4.73 ± 1.78 | 0.002* |
| Adrenal-to-liver ratio | 1.19 ± 0.31 | 1.62 ± 0.52 | 0.009* |

Statistical analysis: *Student t-test; ^Mann–Whitney U test. Min, minimum; Max, maximum; SD, standard deviation; CT, computed tomography; HU, Hounsfield units; SUVmax, maximum standardized uptake value.

**Table 4.** Comparison of SUVmax in avid adrenal lesion group and SUVmax receiver operating characteristic analysis

| Parameter | Area under curve (95% CI) | Cut-off value | Sensitivity (%) | Specificity (%) | *P* value |
|---|---|---|---|---|---|
| **SUVmax (Metastasis and lipid-poor adenomas)** | 0.978 (0.959–1) | > 8.4 | 88% | 99% | < 0.001 |
| **SUVmax (metastasis and non-lipid-poor adenomas)** | 0.993 (0.984–1) | > 5.4 | 95% | 99% | < 0.001 |
| **Adrenal-to-liver ratio (Metastasis and lipid-poor adenomas)** | 0.990 (0.972–1) | > 2.60 | 88% | 99% | < 0.001 |
| **Adrenal-to-liver ratio (Metastasis and non-lipid-poor adenomas)** | 0.999 (0.998–1.00) | > 1.8 | 99% | 99% | < 0.001 |
| **SUVmax (metastasis and all adenomas)** | 0.990 (0.978–1) | > 5.5 | 95% | 98% | < 0.001 |
| **Adrenal-to-liver ratio (Metastasis and all adenomas)** | 0.998 (0.994–1) | > 1.8 | 99% | 98% | < 0.001 |

CI, confidence interval; SUVmax, maximum standardized uptake value.

specificity in the evaluation of adrenal lesions, its complementary role alongside CT and MRI should not be overlooked, particularly in the characterization of lipid-poor adenomas and small-sized metastatic lesions.[19,20]

Each imaging modality has distinct strengths and limitations. Unenhanced CT is highly specific for non-lipid-poor adenomas but is less effective for lipid-poor lesions. Although washout CT was helpful in certain indeterminate cases, its discriminative ability was inferior to PET-based parameters in our cohort. In lesions with attenuation values > 10 HU, chemical-shift MRI is strongly recommended due to its higher sensitivity for detecting intracellular lipid, particularly in lipid-poor adenomas.[20] FDG PET/CT provides valuable metabolic information and high sensitivity for malignancy; however, it is susceptible to false-positive findings in lipid-poor adenomas and false-negative results in certain low-grade malignancies. In cases where diagnostic uncertainty persists, FDG PET/CT remains a clinically valuable problem-solving tool.[12,21,22]

In summary, lipid-poor adenomas are metabolically more active and demonstrate higher SUVmax values than non-lipid-poor adenomas, creating a significant diagnostic challenge. Accurate differentiation is optimized when metabolic information from FDG PET/CT is integrated with CT attenuation values and chemical-shift MRI findings. This multimodality imaging strategy significantly improves diagnostic accuracy in distinguishing benign from malignant adrenal lesions and represents the most reliable approach for managing indeterminate adrenal lesions.[23]

This study has several limitations. First, its retrospective design limited the availability of complete clinical, biochemical, and histopathological confirmation for all patients. Second, not all adrenal lesions were pathologically confirmed, and diagnoses in some cases relied on imaging features and follow-up stability, which may have influenced diagnostic accuracy. Third, imaging was performed over an extended period, during which CT, MRI, and PET/CT acquisition protocols and reconstruction techniques evolved. This long study interval introduced heterogeneity in PET/CT technology that may have affected SUV measurements, despite normalization strategies.

In conclusion, our results demonstrate that lipid-poor adenomas show significantly higher FDG uptake than non-lipid-poor adenomas, frequently exceeding commonly used PET thresholds and thereby representing a potential diagnostic pitfall. Because lesion categorization in our study was primarily based on MRI features, our findings highlight that metabolic activity on PET/CT may overlap between adenoma subtypes already considered indeterminate on MRI. This overlap underscores a persistent diagnostic dilemma in the characterization of lipid-poor adrenal lesions.

### Footnotes

### Conflict of interest disclosure

Şükrü Mehmet Ertürk, MD, is Editor-in-Chief of Diagnostic and Interventional Radiology. He had no involvement in the peer review of this article and had no access to information regarding its peer review. The other authors declared no conflicts of interest.

## References


1. Glazer DI, Mayo-Smith WW. Management of incidental adrenal masses: an update. *Abdom Radiol (NY)*. 2020;45(4):892-900. [Crossref]
2. Blake MA, Holalkere NS, Boland GW. Imaging techniques for adrenal lesion characterization. *Radiol Clin North Am*. 2008;46(1):65-78. [Crossref]
3. Schieda N, Siegelman ES. Update on CT and MRI of adrenal nodules. *AJR Am J Roentgenol*. 2017;208(6):1206-1217. [Crossref]
4. Israel GM, Korobkin M, Wang C, Hecht EN, Krinsky GA. Comparison of unenhanced CT and chemical shift MRI in evaluating lipid-rich adrenal adenomas. *AJR Am J Roentgenol*. 2004;183(1):215-219. [Crossref]
5. Boland GW, Dwamena BA, Jagtiani Sangwaiya M, et al. Characterization of adrenal masses by using FDG PET: a systematic review and meta-analysis of diagnostic test performance. *Radiology*. 2011;259(1):117-126. [Crossref]
6. Outwater EK, Siegelman ES, Huang AB, Birnbaum BA. Adrenal masses: correlation between CT attenuation value and chemical shift ratio at MR imaging with in-phase and opposed-phase sequences. *Radiology*. 1996;200(3):749-752. [Crossref] Erratum in: *Radiology*. 1996;201(3):880.
7. Caoili EM, Korobkin M, Francis IR, Cohan RH, Dunnick NR. Delayed enhanced CT of lipid-poor adrenal adenomas. *AJR Am J Roentgenol*. 2000;175(5):1411-1415. [Crossref]
8. Elsherif SB, Javadi S, Blair KJ, et al. Preresection radiologic assessment and imaging features of 156 pathologically proven adrenal adenomas. *J Comput Assist Tomogr*. 2020;44(3):419-425. [Crossref]
9. Mitchell DG, Crovello M, Matteucci T, Petersen RO, Miettinen MM. Benign adrenocortical masses: diagnosis with chemical shift MR imaging. *Radiology*. 1992;185(2):345-351. [Crossref]
10. Tu W, Verma R, Krishna S, McInnes MDF, Flood TA, Schieda N. Can Adrenal adenomas be differentiated from adrenal metastases at single-phase contrast-enhanced CT? *AJR Am J Roentgenol*. 2018;211(5):1044-1050. [Crossref]
11. Boland GW, Lee MJ, Gazelle GS, Halpern EF, McNicholas MM, Mueller PR. Characterization of adrenal masses using unenhanced CT: an analysis of the CT literature. *AJR Am J Roentgenol*. 1998;171(1):201-204. [Crossref]
12. Hamrahian AH, Ioachimescu AG, Remer EM, et al. Clinical utility of noncontrast computed tomography attenuation value (Hounsfield units) to differentiate adrenal adenomas/hyperplasias from nonadenomas: Cleveland Clinic experience. *J Clin Endocrinol Metab*. 2005;90(2):871-877. [Crossref]
13. Outwater EK, Blasbalg R, Siegelman ES, Vala M. Detection of lipid in abdominal tissues with opposed-phase gradient-echo images at 1.5 T: techniques and diagnostic importance. *Radiographics*. 1998;18(6):1465-1480. [Crossref]
14. Aldhufian M, Sheinis Pickovsky J, Alfaleh H, Melkus G, Schieda N. Prevalence of 'Fat-Poor' adrenal adenomas at chemical-shift MRI. *Can Assoc Radiol J*. 2024;75(1):98-106. [Crossref]
15. Sebro R, Aslam R, Muglia VF, Wang ZJ, Westphalen AC. Low yield of chemical shift MRI for characterization of adrenal lesions with high attenuation density on unenhanced CT. *Abdom Imaging*. 2015;40(2):318-326. [Crossref]
16. Launay N, Silvera S, Tenenbaum F, et al. Value of 18-F-FDG PET/CT and CT in the diagnosis of indeterminate adrenal masses. *Int J Endocrinol*. 2015;2015(1):213875. [Crossref]
17. Murayama R, Nishie A, Hida T, et al. Uptake of 18F-FDG in adrenal adenomas is associated with unenhanced CT value and constituent cells. *Clin Nucl Med*. 2019;44(12):943-948. [Crossref]
18. Dong A, Cui Y, Wang Y, Zuo C, Bai Y. (18) F-FDG PET/CT of adrenal lesions. *AJR Am J Roentgenol*. 2014;203(2):245-252. [Crossref]
19. Metser U, Miller E, Lerman H, Lievshitz G, Avital S, Even-Sapir E. 18F-FDG PET/CT in the evaluation of adrenal masses. *J Nucl Med*. 2006;47(1):32-37. [Crossref] /
20. Chung R, Garratt J, Remer EM, et al. Adrenal neoplasms: lessons from adrenal multidisciplinary tumor boards. *Radiographics*. 2023;43(7):e220191. [Crossref]
21. He X, Caoili EM, Avram AM, Miller BS, Else T. 18F-FDG-PET/CT Evaluation of indeterminate adrenal masses in noncancer patients. *J Clin*

*Endocrinol Metab*. 2021;106(5):1448-1459. [Crossref]

22. Haider MA, Ghai S, Jhaveri K, Lockwood G. Chemical shift MR imaging of hyperattenuating (>10 HU) adrenal masses: does it still have a role? *Radiology*. 2004;231(3):711-716. [Crossref]

23. Chong S, Lee KS, Kim HY, et al. Integrated PET-CT for the characterization of adrenal gland lesions in cancer patients: diagnostic efficacy and interpretation pitfalls. *Radiographics*. 2006;26(6):1811-1824. [Crossref] Erratum in: *Radiographics*. 2007;27(6):1594.